S-glycosyltransferase UGT74B1 can glycosylate both S- and O-acceptors: mechanistic insights through substrate specificity

P. Lafite, Sami Marroun, Gaël Coadou, S. Montaut, S. Marques, M. Schuler, P. Rollin, A. Tatibouët, R. Daniellou, Hassan Oulyadi

S-Glycosyltransferase UGT74B1 can glycosylate both *S*- and *O*-acceptors: mechanistic insights through substrate specificity.

P. Lafite[1,†,*], S. Marroun[2,†], G. Coadou[2], S. Montaut[3], S. Marquès[1], M. Schuler[1], P. Rollin[1], A.Tatibouët[1], R. Daniellou[1,§], H. Oulyadi[2,§].

[1] ICOA, Université d'Orléans, CNRS, UMR 7311, BP6759 Rue de Chartres, F-45067 Orléans Cedex 2, France.

[2]Normandie Univ, COBRA, UMR 6014 / FR 3038; Univ Rouen; INSA Rouen; CNRS, IRCOF, 1 rue Tesnière, 76821 Mont Saint Aignan Cedex, France.

[3]Department of Chemistry and Biochemistry, Biomolecular Sciences Programme, Laurentian University, 935 Ramsey Lake Road, Sudbury, ON P3E 2C6, Canada.

To whom correspondence should be addressed: Pierre Lafite, ICOA UMR CNRS 7311, Université d'Orléans, FR-45067, France. pierre.lafite@univ-orleans.fr ; Tel.(+33) 238494855

[†] : both authors contributed equally to this work. [§] : these 2 authors are co last authors.

Abstract

UGT74B1 from *Arabidopsis thaliana* is one of the few characterized glycosyltransferases able to generate a thioglycosidic linkage *in vivo,* using the sulfur atom of thiohydroximate as the nucleophile in the glycosylation reaction. This critical biosynthetic step in glucosinolate production has been documented. Yet little is known about the molecular mechanism that enables this rare and unusual glycosylation at the sulfur atom. To identify the role of this atom in the glycosylation reaction and unraveling the mechanism of UGT74B1, we used a range of substrates containing either sulfur or oxygen. We first demonstrated that the enzyme could catalyze the glycosylation of thiohydroximates but also of *O*-containing hydroximate analogs. If K_M values were shown to be close between analogs, the reaction catalytic rate k_{cat} was 50-100 lower in the case of hydroximates. The glycosylation reaction is catalyzed through deprotonation of the acceptor, which was confirmed by the removal of catalytic carboxylic residues by site-directed mutagenesis. Moreover, using a range of simple phenols and thiophenols as UGT74B1 substrate acceptors for glycosylation, we concluded that the glycosylation reaction rate is correlated to the acceptor atom acidity, and not to the nature of this nucleophilic atom (oxygen or sulfur).

Graphical Abstract

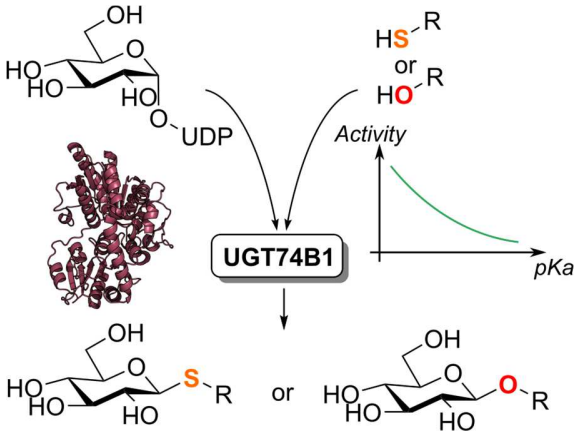

Keywords

Glucosyltransferase, glycosylation, enzyme mechanism, sulfur, *Arabidopsis thaliana*

Abbreviations

GT, Glycosyltransferase; PATH: Phenylacetothiohydroximate; PPTH: Phenylpropanothiohydroximate; PAH: Phenylacetohydroximate; PPH: Phenylpropanohydroximate; CTP: Chlorothiophenol; TP: Thiophenol; TCP: Trichlorophenol; DCP: Dichlorophenol; CP: Chlorophenol.

1. Introduction

Glycosyltransferases (GT) (EC: 2.4.x.x) catalyze the transfer of a sugar from an activated donor to an acceptor [1]. Nucleotide-sugar utilizing GTs, known as Leloir enzymes, are the most abundant group, and the molecular mechanisms that lead to the formation of the glycosidic [2] bond have been widely studied, for retaining or inverting GTs, considering the stereochemistry of the anomeric carbon of the glycoside [3]. In the case of inverting GTs, a SN_2 reaction takes place, involving a single displacement step with the formation of an oxocarbenium ion-like transition state. Moreover, a catalytic base residue located in the active site can generally increase the nucleophilicity of the acceptor-attacking atom to generate the glycosidic linkage.

Whereas the canonical *O*- and *N*-glycoconjugates are involved in a wide range of biological processes, [4,5] the more unusual *S*- or *C*-glycosides also exhibit many biological roles, for instance in protein glycosylation [6]. Moreover, the nature of the atom in the glycosidic linkage can influence the chemical and physical properties of the glycoconjugates. Especially, *S*-glycosides are of particular interest because they are structural analogs of their *O*-counterparts, while being much more resistant to chemical and/or enzymatic hydrolysis [7–10]. However, though GT engineering has been extensively investigated to increase substrate promiscuity and specificity towards sulfur containing acceptors [11–14], little is known still about the influence of the nucleophilic atom on substrate specificity. Even though several examples of GTs exhibiting dual or triple activity with either *O*-, *S*-, *N*-, or *C*-containing acceptors have been reported [15–22], the molecular mechanism underlying this promiscuity was never discussed. However, Gutmann *et al.* have managed to identify active site motifs that could turn an *O*-GT into a *C*-GT [23,24].

In this context, we have recently reported the UDP-sugar donor specificity of UGT74B1, making this versatile GT a strong candidate for biosynthesis of *S*-glycoconjugates [25]. Along with ThuS and SunS, involved in *S*-glycosylation of bacteriocin peptides [26–29], UGT74B1 from *Arabidopsis thaliana* is one of the only *S*-GTs involved in the natural biosynthesis of the most historically known *S*-glycosides, namely glucosinolates [30,31]. Herein, we have studied UGT74B1 and identified the mechanism that leads to its specificity for *S*-glycosylation *versus O*-glycosylation, using a diverse panel of acceptor substrates.

2. Materials and methods

2.1 Chemicals

All used chemicals and buffers were of the highest purity available. HPLC solvents, phenols, thiophenols, pyruvate kinase, lactate dehydrogenase, phosphoenolpyruvate, NADH were purchased from Sigma-Aldrich (Merck). Molecular biology and microbiology chemicals were purchased from ThermoFisher. UDP-α-D-glucose was obtained from Carbosynth Ltd (UK).

^{1}H NMR and ^{13}C NMR spectra of synthesized compounds were recorded on Bruker Avance II 400 or Bruker DPX 250 spectrometers. Assignments are based on DEPT 135 sequence and on homo- and heteronuclear correlations. Chemical shifts are reported in parts per million (ppm) from tetramethylsilane as the internal standard. Coupling constants (J) are reported and expressed in Hertz (Hz); splitting patterns are designed as br (broad), s (singlet), d (doublet), dt (doublet of triplets), t (triplet) and m (multiplet). High-resolution mass spectra (HRMS) were obtained with a Maxis Bruker 4G instrument from the "Fédération de Recherche" ICOA/CBM (FR2708) platform in the electrospray ionization (ESI) mode. Infrared spectra of compounds were recorded with a Thermo Scientific Nicolet iS10 spectroscope.

Preparation of PAH and PPH was adapted from published literature [32]. 1,1'-Carbonyldiimidazole (1.2 equiv.) was added to phenylpropanoic acid or phenylacetic acid (6 mmol, 1 equiv.) dissolved in CH_3CN (20 mL) under argon atmosphere and the mixture was stirred at 22 °C for 1h. A solution of NH_2OH (50 wt. % in H_2O, 2 ml, 5 equiv.) was then added and the reaction mixture was stirred at 22 °C for 20h. After concentration under reduced pressure, H_2O (15 mL) was added to the residue and the aqueous solution was extracted with EtOAc (3 x 15 mL). The combined organic phase was washed with brine (1 x 25 mL), dried over Na_2SO_4, filtered and evaporated under reduced pressure. The residue was purified by Reveleris® column chromatography on C18 silica gel (H_2O 100% to CH_3CN 100%) to afford the desired products as a slightly greenish powders.

PAH (Figure S1): 682 mg, 75% yield. ^{1}H NMR (250 MHz, DMSO-d_6): δ 10.59 (s, 1H, OH), 8.77 (s, 1H, NH), 7.28-7.14 (m, 5H, H-Ar), 3.26 (s, 2H, CH_2).[33,34]

PPH (Figure S2): 761 mg, 65% yield). ^{1}H NMR (400 MHz, DMSO-d_6): δ 10.36 (s, 1H, OH), 8.70 (s, 1H, NH), 7.27-7.17 (m, 5H, H-Ar), 2.80 (t, 2H, J = 7.7 Hz, H-3), 2.25 (t, 2H, J = 7.7 Hz, H-2). [33,34].

2.2 1.2 Cloning and expression of UGT74B1.

UGT74B1 was cloned as a histidine-tagged protein in *E. coli* and purified as previously reported [25]. Site-directed mutagenesis were carried out using QuikChange II XL Site-Directed Mutagenesis kit (Agilent) using WT-UGT74B1 plasmid as DNA template. Primers used for site-directed mutagenesis are presented in Table S1 in Supplementary data. Mutagenesis products were directly transformed into XL10-Gold ultracompetent cells (Agilent) by heat shock method. Each mutant sequence DNA was sequenced (Eurofins genomics) and confirmed to be identical to the known wild-type enzyme sequence DNA except the targeted codon (either His22 and Asp113) replaced by alanine.

2.3 Enzymatic assay (Enzyme-coupled)

Determination of enzymatic glycosylation for thiohydroximates PATH, PPTH and hydroximates PAH, PPH were done using a tri-enzymatic assay that couples UDP formation with NADH consumption, using

pyruvate kinase and lactate dehydrogenase as enzymatic mixture. Reactions conditions were identical to those reported previously [25]. Kinetics data were analyzed and fitted using Prism 4 (GraphPad).

2.4 Enzymatic assay (HPLC separation)

For thiophenols and phenols, an HPLC separation methodology was used to quantify enzymatic activity. A reaction (200 µL total volume) containing 1mM UDP-glucose, acceptor (20 µL in 100% MeOH – final concentrations ranging from 50 to 5000 µM) in 20 mM Tris buffer pH 8.0 was started by addition of 1 µM UGT74B1. The reaction was left for 15 min at 37°C, then 200 µL of quenching reagent (CH_3CN:HCOOH, 10:1) was added to the mixture. Proteins were precipitated by centrifugation for 10 min at 10,000 rpm, and the supernatant was analyzed by reverse-phase HPLC on a Zorbax Eclipse XDB-C18 column 4.6 × 150 mm (Agilent) on an Agilent 1220 Infinity II LC System. The mobile phase was delivered at a rate of 1 mL/min with a gradient from A (0.1% HCOOH in H_2O) to B (0.1% HCOOH in CH_3CN) (10% B for 4 min, 10% to 60% B in 10 min, 60% to 100% B in 2 min.). The column effluent was monitored at 250 nm.

2.5 NMR structural study of desulfo-glucotropaelin

NMR spectra of glucosylated PATH product were recorded in DMSO-d_6 solution at 313K on a Bruker AVIII 500 spectrometer operating at 500.13 MHz for ^{1}H and 125.13 MHz for ^{13}C. 1D and 2D experiments (1D ^{1}H, 2D ^{1}H-^{1}H COSY, ^{1}H-^{1}H NOESY, ^{1}H-^{13}C HMQC and HMBC) were run under TopSpin (version 3.2, Bruker Biospin, Karlsruhe) with a BBFO {^{1}H, X} probe and a z gradient coil giving a maximum gradient of 50 G cm^{-1}. ^{1}H and ^{13}C chemical shifts were referenced to the solvent residual signals of DMSO-d_6 (δ 2.49 for ^{1}H and 39.70 ppm for ^{13}C).

2.6 Saturation transfer difference

STD spectra of the mixture of UGT74B1 (100µM) with UDPG (1 mM) in phosphate buffer pH=7.3 were undertaken on a Bruker Avance III 600 equipped with CPTXI-cryoprobe. The experiments were acquired with the standard Bruker stddiffesgp.3 sequence by using trains of E-Burp-1 90° selective pulses. Selective pulses were applied at 0 ppm for the on resonance STD excitation, and -17.00 ppm for the difference spectrum, with respect to H_2O at 4.70 ppm. The spectra were measured with 8080 scans after eight dummy scans and lasted approximately 39 hours.

2.7 pKa determination by NMR

Thiohydroxamic and hydroxamic acids, and CTP were first characterized by NMR on a Bruker Avance III 600 equipped with a CPTXI-cryoprobe. Then, ^{1}H chemical shifts of these compounds were monitored for pH in order to determine their pKa in a 90:10 mixture of phosphate buffer pH 7.3 and methanol (CD_3OH). The method consists of making 1D ^{1}H acquisitions following successive additions of acid or base. Labile

protons are not detectable under these experimental conditions (phosphate buffer) because they undergo rapid exchange. The chemical shift of the Hα protons closest to the deprotonation site is the one which is followed by this method. A titration curve was established by following the chemical shift of the chosen proton as a function of the pH. The obtained data were fitted with an asymmetrical sigmoidal function, which gave the value of the pKa.

2.8 pKa calculations

Phenols and thiophenols pKa were calculated using ACD/Labs software.

3. Results

3.1 UGT74B1 is able to glycosylate O-acceptors

Phenylacetothiohydroximate (PATH) and phenylpropanothiohydroximate (PPTH) (Fig. 1.A) were prevsiously reported to undergo efficient *S*-glycosylation, with second order catalytic rate k_{cat}/K_M above 10^5 $min^{-1}.mM^{-1}$ (Table 1) [25]. The *O*-containing analogues of PATH and PPTH, respectively phenyacetohydroximate (PAH) and phenylpropanohydroximate (PPH) were synthesized using slightly modified reported methods [32]. Both hydroximates were used in UGT74B1 glycosylation assays following the same procedure, and their catalytic constants were determined (Table 1). Both *O*-acceptors have µM range K_M similar to those calculated for thiohydroximates PATH and PPTH. However, the catalytic turnover is dramatically decreased when swapping the sulfur atom for the oxygen atom, as k_{cat} of a hydroximate is 100-fold lower than the one for the corresponding thiohydroximate. UGT74B1 can thus bind hydroximates as efficiently as thiohydroximates, as K_M values lie in the same order of magnitude. However, the reactivity of the oxygen atom in hydroximates is much lower than that of sulfur atom in PATH and PPTH, yielding lower catalytic rate k_{cat} and catalytic efficiency k_{cat}/K_M.

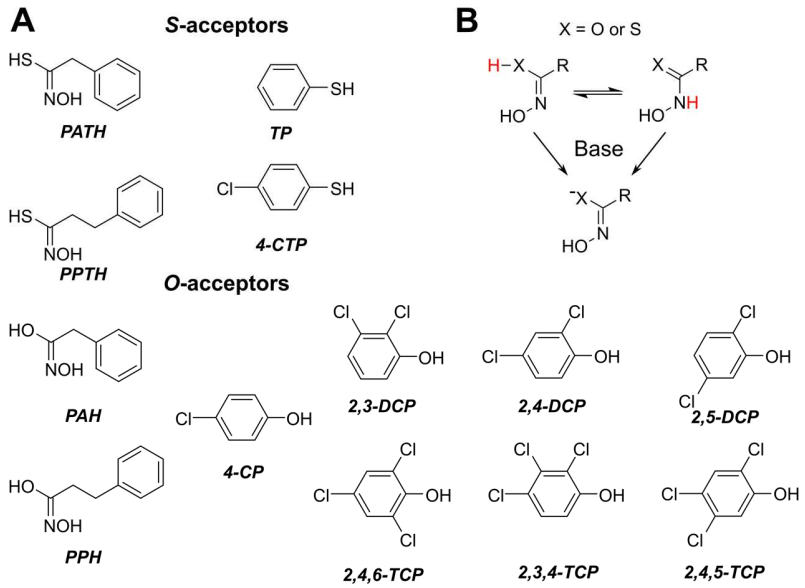

Figure 1: ***(A)*** UGT74B1 substrates used in this study. ***(B)*** Tautomeric equilibrium and deprotonation of thiohydroximates and hydroximates.

UGT74B1 variant	**Acceptor**	K_M (µM)	k_{cat} (min^{-1})	k_{cat}/K_M ($min^{-1}.mM^{-1}$)
Wild-type	**PATH**[a]	3.1 ± 0.6	280 ± 58	90 x 10^3
	PPTH[a]	2.2 ± 0.5	326 ± 95	148 x 10^3
	PAH	1.1 ± 0.2	3.9 ± 1.3	3.5 x 10^3
	PPH	0.9 ± 0.2	4.3 ± 1.2	4.8 x 10^3
His22Ala	**PATH**	*n.d.*[b]	*n.d.*	*n.d.*
	PPTH	*n.d.*[b]	*n.d.*	*n.d.*
Asp113Ala	**PATH**	27.2 ± 4.5	1.2 ± 0. 1[c]	
	PPTH	58.9 ± 11.4	2.4 ± 0.1[c]	

Table 1: Catalytic constants of UGT74B1 (wild-type and mutated) towards thiohydroxamic and hydroxamic acids. Values were obtained at 37°C, pH 8.0. *PATH : Phenylacetothiohydroximate ; PPTH : Phenylpropanothiohydroximate ; PAH : Phenylacetohydroximate ; PPH : Phenylpropanohydroximate.* [a] *From reference 31.* [b]*n.d. non detectable.* [c]*: Vmax in µM.min*$^{-1}$

3.2 UGT74B1 requires an acidic acceptor

UGT74B1 belongs to the CAZy GT1 family [35], and we have previously built an homology model using several GT1 templates, and identified residues surrounding the active site [25]. A NMR structural

study of glucosylated PATH (namely desulfo-glucotropaelin [25,36]) product solution was undertaken in DMSO-d_6 (Fig S3-S7). This allowed for a complete assignment of protons signals for desulfo-glucotropaelin, showing reverse anomeric carbon stereochemistry between UDP-α-D-glucose donor and product confirming the mechanism predicted by the homology model. Moreover, a Saturation Transfer Difference (STD) experiment was used to probe UDP-α-D-glucose binding to UGT74B1. In this experiment, the signals of the UDP-α-D-glucose atoms are modulated in intensity depending on how closely they bind to UGT74B1 (Fig. 2). The relative ranking of this modulation shows that UDP-α-D-glucose is strongly bound to UGT74B1 by its aromatic base and less by its glucosyl moiety. This result is in full agreement with binding modes predicted through molecular docking where the aromatic ring is stabilized by a strong and close range π-stacking interaction [25].

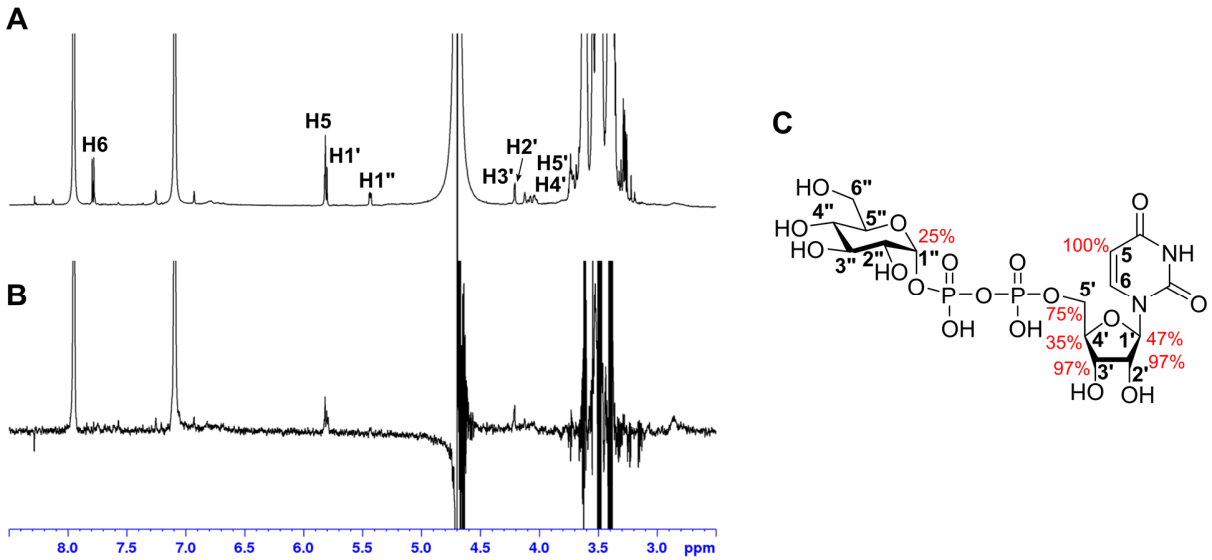

Figure 2: (A) 1D ^{1}H NMR spectrum of the mixture of UGT74B1 and UDP-α-D-glucose and (B) the corresponding STD-NMR (600MHz, T=298K, phosphate buffer pH 7.3). (C) Epitope mapping of UDP-α-D-glucose.

Like most GT1 reported structures, UGT74B1 exhibits a catalytic dyad formed of a carboxylic acid amino acid (Asp113) in close contact with an histidine (His22), which is located in the suitable distance to deprotonate the acceptor (Fig. 3). It has to be noted that hydroximates and thiohydroximates can exist under two tautomeric forms (Fig 1.B). Yet, deprotonation of both tautomers will eventually lead to the nucleophilic attack of either oxygen or sulfur, depending on the substrate considered. This mechanism is similar to the triad observed in a serine protease mechanism. Both residues were also identified as the potential catalytic dyad in the homology model built by Kopycki *et al.* [31]. However the role of these residues is still unclear as some GT1 do not possess these two amino acids [37] and several studies have demonstrated that unlike

O-glycosylation, the histidine residue was not involved catalytically in *N*-glycosylation reactions [16,38]. In contrast to hydroxyl that needs to be deprotonated to avoid the formation of a highly unstable positively charged oxonium ion (R1-OH$^+$-R2), amines can readily form a positively charged intermediate without preliminary deprotonation [16]. In order to elucidate the role of these two residues in the catalytic mechanism of UGT74B1, we have generated two mutants in which either His22 or Asp113 were replaced with the non-reactive alanine.

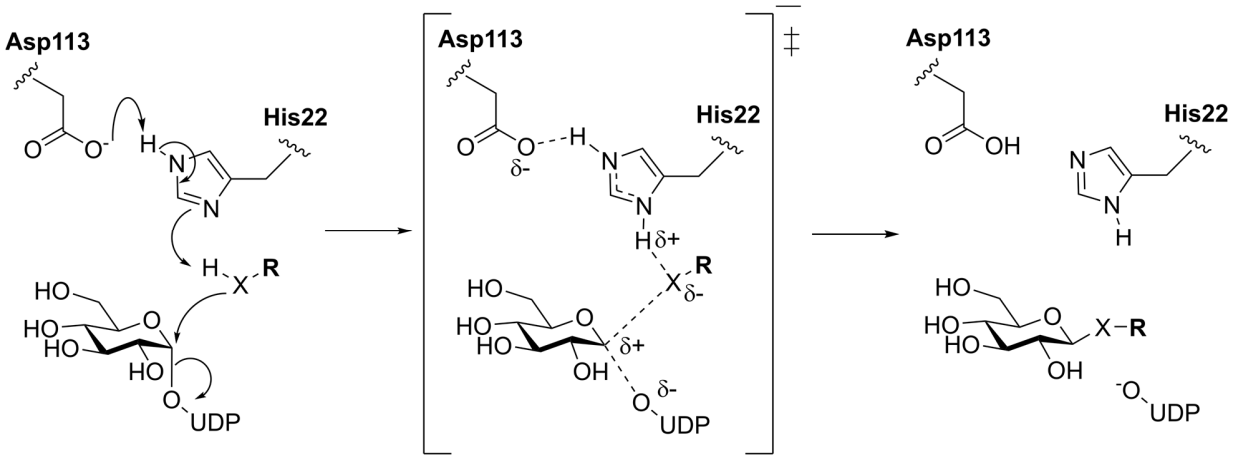

Figure 3: Proposed SN_2 mechanism of glycosylation reaction catalyzed by UGT74B1 (X=O or S). *Asp113 and His22 are depicted as putative components of the catalytic dyad, as identified with the homology model of UGT74B1.*

Both mutants were expressed and purified. However Asp113Ala could not be purified to homogeneity on Immobilized Metal-Affinity Chromatography column, unlike His22Ala that could be purified in quantity as high as WT UGT74B1 (typically 10 mg. l^{-1} culture) (Fig. S8-A). His22Ala mutation abolished enzymatic activity, as no activity could be detected in our assay (Fig. S8-B). This indicates that this residue is critical to deprotonate thiol acceptors before the nucleophilic attack (like in other GT1 *O*-glycosylation mechanism).

Unlike His22, the contribution of Asp113 in promoting this deprotonation is unclear as Asp113Ala mutant still exhibited enzymatic activity. The Michaelis Menten fit of PATH or PPTH concentration dependence (Fig. S8-B) gave respective Michaelis constants K_M of 27 µM and 59 µM, higher than the value calculated for WT UGT74B1 (Table 1). However, the catalytic turnover k_{cat} could not be determined, as Asp113Ala mutant could not be obtained as a pure enzyme. Maximum velocity V_{max} was determined to be 1.2 and 2.4 µM.min^{-1}for each substrate, indicating that Asp113Ala residual activity is not insignificant, considering the low amount of impure enzyme introduced in the reaction mixture.

These mutation studies indicated that the acceptor acidity is crucial in UGT74B1 activity, and to assess this hypothesis we determined the pKa of sulfur- (PATH, PPTH) and oxygen- (PAH, PPH) containing

acceptors. Concerning pKa values, no recent data were available for thiohydroximates in the literature [39]. Acidity constants of all four substrates were thus determined by NMR.

Protons located on the alpha-carbon (Hα) of the 4 substrates were used as probes for pKa determination (Fig. 4-A). Chemical shifts of both protons were determined in a range of buffered solutions, and plotting of δ=f(pH) gave a sigmoidal curve fitting, which inflexion point corresponding to experimental pKa (Fig. 4-B). This methodology was successfully used for other acidity constant determinations [40,41]

The calculated values for all 4 substrates were PATH: 4.4; PPTH: 4.6; PAH: 9.2; PPH: 9.4. (See Fig. S9 to S11) The values for thiohydroximates, are close to those (between 4.0 and 5.6) reported by Nagata *et al.* [39].

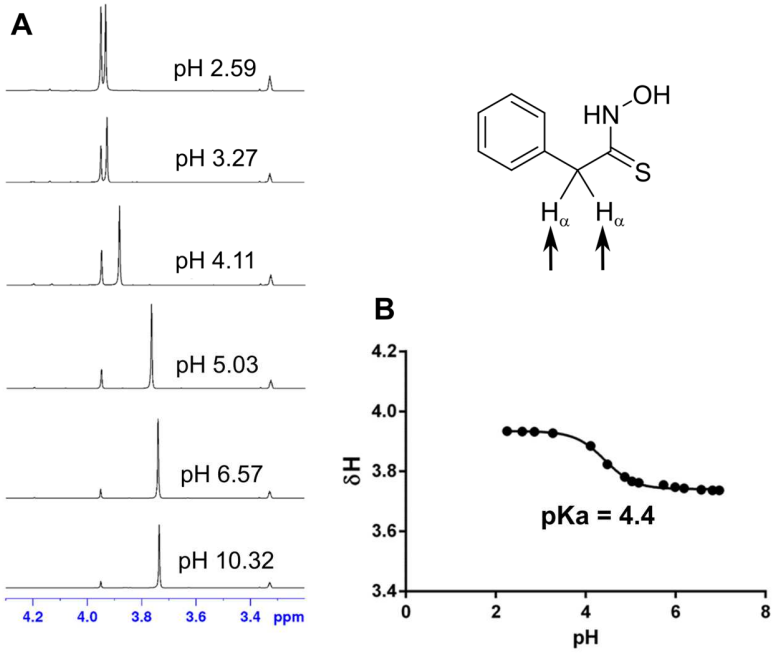

Figure 4: PATH pKa determination by *NMR. (A) ^{1}H NMR spectrum of PATH. Arrow indicates protons and corresponding signals used for pKa determination. (B) Evolution of chemical shift with pH and pKa determination.*

3.3 GT activity is correlated to the pKa of the nucleophile acceptor

pKa comparison of thiohydroximates and hydroximates indicates that a low pKa (PATH and PPTH) gives a higher enzymatic activity than a high pKa (PAH and PPH). This can be understood as thiohydroximates can easily form the corresponding thiolates after His22 deprotonation, and thus are more reactive than their hydroximate counterparts. However, because the pKa values do not cover a wide range

of values (pKa values gap between 5 and 9), the correlation between pKa and enzymatic activity is not obvious.

To evaluate this potential correlation, we have used simple acceptors, that cover a more extended pKa range (Fig. 1 and Table 2). The selected compounds were *O*-containing chloro-substituted phenols (4-chlorophenol CP, 2,3- 2,4- and 2,5 dichlorophenols DCP, 2,3,4- 2,4,5- 2,4,6- trichlorophenols TCP) and *S*-containing thiophenols (4-chlorothiophenol CTP and thiophenol TP), presenting a calculated pKa range between 5.5 and 9.0. To validate the *in silico* calculation of pKa, pKa determination by NMR was applied to CTP (Fig. S12), giving a value similar to the calculated value (respectively 5.8 and 5.5).

Acceptor	pKa[a]	K_M (µM)	k_{cat} (min^{-1})	k_{cat}/K_M ($min^{-1}.mM^{-1}$)
PATH	4.4 [a]	3.1 ± 0.6	280 ± 58	90 x 10^3
PPTH	4.6[a]	2.2 ± 0.5	326 ± 95	148 x 10^3
PAH	9.2[a]	1.1 ± 0.2	3.9 ± 1.3	3.5 x 10^3
PPH	9.4[a]	0.9 ± 0.2	4.3 ± 1.2	4.8 x 10^3
4-CTP	5.8[a]/5.5[b]	215 ± 13	139.0 ± 5.6	647
TP	6.6[b]	105 ± 24	10.9 ± 1.5	104
2,4,6-TCP	6.0[b]	132 ± 24	14.5 ± 1.3	110
2,4,5-TCP	6.8[b]	130 ± 45	6.1 ± 1.1	47
2,3,4-TCP	7.0[b]	147 ± 6	6.6 ± 0.9	45
2,5-DCP	7.2[b]	132 ± 23	4.2 ± 0.2	32
2,3-DCP	7.4[b]	195 ± 26	1.9 ± 0.3	10
2,4-DCP	7.4[b]	148 ± 5	2.2 ± 0.3	15
4-CP	9.0[b]	149 ± 43	0.6 ± 0.2	3

Table 2: Catalytic constants and pKa of thiohydroxamic acids, hydroxamic acids, phenol and thiophenol derivatives. Values were obtained at 37°C, pH 8.0. *[a]measured by NMR; [b] calculated using ACD/Labs. CTP: Chlorothiophenol; TP: Thiophenol; TCP: Trichlorophenol; DCP: Dichlorophenol; CP: Chlorophenol.*

Because of their lower solubility, phenols can interfere with the tri-enzymatic assay used that couples UDP formation by UGT74B1 with NADH consumption. The latter is determined spectrophotometrically at 340 nm. We have set up an activity assay based on HPLC separation of phenols and the corresponding glycosylated products. When validated by using PATH and PPTH as substrates, this assay gave similar catalytic constants as those presented in Table 1 (data not shown).

All eight phenols and thiophenols where used as acceptors in UGT74B1 reaction, and their catalytic constants where determined (Table 2). All compounds are glycosylated by UGT74B1 when using UDP-α-

glucose as sugar donor. They all exhibit similar K_M values (100-200 µM), higher than those determined for hydroximates or thiohydroximates, probably because phenols might establish less stabilizing interactions in UGT74B1 active site. The observed rates fit those reported by Braziers-Hicks *et al.*, as 2,4,5-TCP is one order of magnitude less active than 4-CTP [16].

The resulting Brønsted analysis of glycosylation provides evidence of a correlation between enzymatic efficiency k_{cat}/K_M and pKa of the acceptor (Fig. 5). Unlike other studies on nucleophile pKa dependence of GT activity [42], the corresponding slope calculated $\beta_{nu=}$-0.64 (R^2=0.91) for UGT74B1 is negative. As β_{nu} value can give an estimate of the change in effective charge on the nucleophile towards the transition state [43], acceptor nucleophilic atoms (*O*- or *S*-) in UGT74B1 have a negative charge accumulation during catalysis, which is in agreement with the transient formation of deprotonated thiolate or hydroxylate during catalysis (Fig. 3)

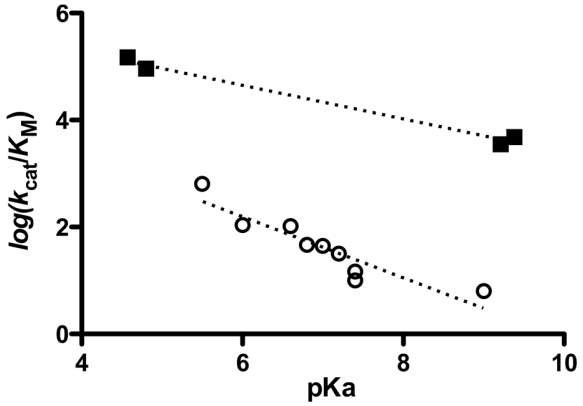

Figure 5: Brønsted plot of k_{cat}/K_M for all tested UGT74B1 substrates. Values for thiohydroxamic and hydroxamic acids are depicted as black squares. Data corresponding to thiophenol and phenol derivatives are marked as white circles.

A similar enzymatic mechanism can be proposed for thiohydroximates and hydroximates, although no data is available between pKa values of 5 and 9. Brønsted analysis gives also a negative slope $\beta_{nu=}$-0.31, although shallower than for phenols. During catalysis, thiohydroximates and hydroximates accumulate less negative charge on nucleophilic atoms, and are more sensitive to general acid/base mechanism than phenols.

In both cases, the Brønsted analyses do not demonstrate that the nature of the nucleophilic atom is critical for catalysis, as there is a continuum in linear correlation – especially for phenolic derivatives.

4. Discussion

In *Brassicaceae* plants, UGT74B1 was originally identified as a key enzyme in the biosynthesis of glucosinolates, catalyzing the *S*-glucosylation of thiohydroximates [30,44]. The enzyme was annotated as a *S*-glycosyltransferase in genomic data, like other GTs where the specificity of atom that form the glycosidic

bond is highlighted [35]. However many GTs have been reported to be able to use acceptors containing diverse nucleophilic atoms, which calls into question the canonic specificity of GTs towards one particular atom [15–22,24].

Nevertheless, the corresponding studies did not dissected in detail the molecular mechanism underlying this broader specificity. More precisely, the influence of nucleophile's nature on enzyme reactivity was not examined into detail.

UGT74B1 was shown to glycosylate *S*- and *O*-containing acceptors, such as hydroximates, the structure of which is closely related to the natural acceptor thiohydroximates. The ratio of catalytic efficiency between both families of analogues is of 2 orders of magnitude (10^5 and 10^3 $min^{-1}.mM^{-1}$ range respectively for thiohydroximates and hydroximates). This catalytic efficiency towards *O*-acceptors is not negligible, as other GT1 enzymes exhibited similar kinetic constants towards their "natural" substrates [16,45]. Thus, UGT74B1 can efficiently catalyze *O*- and *S*-glycosylation *in vitro* when using appropriate acceptors, but is solely catalyzing the latter *in vivo* because only endogenous thiohydroximates are efficiently binding to the enzyme and exhibit low pKa.

To assess this versatility of UGT74B1 towards *O*- and *S*-acceptors, a range of chloro-substituted thiophenols and phenols were also used as substrates by UGT74B1. More interestingly, when plotting the logarithm of the second order rate k_{cat}/K_M vs. pKa values of (thio)phenols, a linear correlation could be fitted, and Brønsted-type relationship was demonstrated, with a negative β_{nu} value (Fig. 5). The acceptor nucleophilic atom shows a decrease in effective charge during the catalysis towards the transition state. A transition state where the proton abstraction by His22 is significantly advanced, whereas the glycosidic bond formation is not, can explain this negative β_{nu} value. As a lower absolute value for β_{nu} value can be estimated in the case of hydroximates and thiohydroximates, these substrates are less prone to general base catalysis by His22 [43,46].

UGT74B1 is not the first example of a GT able to generate several glycosidic linkages, when considering the nature of the atom involved in the bond. However, the Brønsted-type relationship for (thio)phenol glycosylation does not exhibit a break between *O*- and *S*- acceptors. The influence of pKa on the reactivity overtakes the nature of the nucleophilic atom. UGT74B1 reactivity is therefore mostly driven by the predisposition of the nucleophile chemical property to be energetically close to the transition state, and thus decreasing the activation energy. The enzyme can accommodate and use several nucleophiles as acceptors, as long as they satisfy the chemistry underlying the catalysis.

The dissected mechanism of UGT74B1 can be used as a paradigm for other GTs able to use several acceptors of similar shape, size, and properties, bearing different nucleophilic atoms, and redefine the conventional nomenclature that classifies a GT according to the nature of the nucleophilic atom.

Acknowledgments & funding sources

The authors thank G. Jousset and A. Duvergé for technical help in producing and characterizing UGT74B1 wild-type and mutants' activities. PL, RD, MS, AT, SMar, GC and HO thank the Labex SynOrg (ANR-11-LABX-0029) for financial support. SMar, GC and HO thank the Région Normandie, CNRS, the University and INSA of Rouen for financial support. SMarq and SMarr were funded by French Ministry of Research.

Declaration of interest

The authors declares that there is no conflict of interest.

References

[1] L.L. Lairson, B. Henrissat, G.J. Davies, S.G. Withers, Glycosyltransferases: Structures, Functions, and Mechanisms, Annu. Rev. Biochem. 77 (2008) 521–555. doi:10.1146/annurev.biochem.76.061005.092322.

[2] K. Xie, R. Chen, J. Li, R. Wang, D. Chen, X. Dou, J. Dai, Exploring the Catalytic Promiscuity of a New Glycosyltransferase from Carthamus tinctorius, Org. Lett. 16 (2014) 4874–4877. doi:10.1021/ol502380p.

[3] A. Ardèvol, C. Rovira, Reaction Mechanisms in Carbohydrate-Active Enzymes: Glycoside Hydrolases and Glycosyltransferases. Insights from ab Initio Quantum Mechanics/Molecular Mechanics Dynamic Simulations, J. Am. Chem. Soc. 137 (2015) 7528–7547. doi:10.1021/jacs.5b01156.

[4] A. Varki, Biological roles of oligosaccharides: all of the theories are correct, Glycobiology. 3 (1993) 97–130. doi:10.1093/glycob/3.2.97.

[5] R.G. Spiro, Protein glycosylation: nature, distribution, enzymatic formation, and disease implications of glycopeptide bonds, Glycobiology. 12 (2002) 43R–56R. doi:10.1093/glycob/12.4.43R.

[6] P. Lafite, R. Daniellou, Rare and unusual glycosylation of peptides and proteins., Nat. Prod. Rep. 29 (2012) 729–38. doi:10.1039/c2np20030a.

[7] R.T. Dere, A. Kumar, V. Kumar, X.M. Zhu, R.R. Schmidt, Synthesis of Glycosylthiols and Reactivity Studies, J Org Chem. 76 (2011) 7539–7545. doi:10.1021/jo200624e.

[8] J.D.C. Codee, R.E.J.N. Litjens, L.J. van den Bos, H.S. Overkleeft, G.A. van der Marel, Thioglycosides in sequential glycosylation strategies, Chem. Soc. Rev. 34 (2005) 769–782. doi:10.1039/B417138C.

[9] H. Driguez, Thiooligosaccharides as Tools for Structural Biology, Chembiochem. 2 (2001) 311–

318. doi:10.1002/1439-7633(20010504)2:5<311::AID-CBIC311>3.0.CO;2-L.

[10] M. Brito-Arias, C-Glycosides, in: Synth. Charact. Glycosides, Springer US, Boston, MA, 2007: pp. 247–271. doi:10.1007/978-0-387-70792-1_5.

[11] A. Chang, S. Singh, G.N. Phillips Jr, J.S. Thorson, Glycosyltransferase structural biology and its role in the design of catalysts for glycosylation, Curr. Opin. Biotech. 22 (2011) 800–808. doi:http://dx.doi.org/10.1016/j.copbio.2011.04.013.

[12] M.M. Palcic, Glycosyltransferases as biocatalysts, Curr. Opin. Chem. Biol. 15 (2011) 226–233. doi:10.1016/j.cbpa.2010.11.022.

[13] S.M. Hancock, M.D. Vaughan, S.G. Withers, Engineering of glycosidases and glycosyltransferases, Curr. Opin. Chem. Biol. 10 (2006) 509–519. doi:10.1016/j.cbpa.2006.07.015.

[14] J. Ati, P. Lafite, R. Daniellou, Enzymatic synthesis of glycosides: from natural O- and N-glycosides to rare C- and S-glycosides, Beilstein J. Org. Chem. 13 (2017) 1857–1865. doi:10.3762/bjoc.13.180.

[15] C. Wen, W. Huang, X.-L. Zhu, X.-S. Li, F. Zhang, R.-W. Jiang, UGT74AN1, a Permissive Glycosyltransferase from Asclepias curassavica for the Regiospecific Steroid 3- O -Glycosylation, Org. Lett. 20 (2018) 534–537. doi:10.1021/acs.orglett.7b03619.

[16] M. Brazier-Hicks, W.A. Offen, M.C. Gershater, T.J. Revett, E.-K. Lim, D.J. Bowles, G.J. Davies, R. Edwards, Characterization and engineering of the bifunctional N- and O-glucosyltransferase involved in xenobiotic metabolism in plants, Proc. Natl. Acad. Sci. U. S. A. 104 (2007) 20238–20243. doi:10.1073/pnas.0706421104.

[17] R.W. Gantt, R.D. Goff, G.J. Williams, J.S. Thorson, Probing the Aglycon Promiscuity of an Engineered Glycosyltransferase, Angew. Chem. Int. Ed. 47 (2008) 8889–8892. doi:10.1002/anie.200803508.

[18] M.L. Falcone Ferreyra, E. Rodriguez, M.I. Casas, G. Labadie, E. Grotewold, P. Casati, Identification of a bifunctional maize C- and O-glucosyltransferase, J. Biol. Chem. 288 (2013) 31678–31688. doi:10.1074/jbc.M113.510040.

[19] Y. Wang, W.-J. Wang, C. Su, D.-M. Zhang, L.-P. Xu, R.-R. He, L. Wang, J. Zhang, X.-Q. Zhang, W.-C. Ye, Cytotoxic quassinoids from Ailanthus altissima, Bioorg Med Chem Lett. 23 (2013) 654–657. doi:10.1016/j.bmcl.2012.11.116.

[20] H. Wang, T.J. Oman, R. Zhang, C. V Garcia De Gonzalo, Q. Zhang, W.A. van der Donk, The glycosyltransferase involved in thurandacin biosynthesis catalyzes both O- and S-glycosylation, J. Am. Chem. Soc. 136 (2014) 84–87. doi:10.1021/ja411159k.

[21] D. Chen, R. Chen, R. Wang, J. Li, K. Xie, C. Bian, L. Sun, X. Zhang, J. Liu, L. Yang, F. Ye, X. Yu, J. Dai, Probing the Catalytic Promiscuity of a Regio- and Stereospecific C-Glycosyltransferase from Mangifera indica, Angew. Chemie. 127 (2015) 12869–12873. doi:10.1002/ange.201506505.

[22] F. Gandia-Herrero, A. Lorenz, T. Larson, I.A. Graham, D.J. Bowles, E.L. Rylott, N.C. Bruce, Detoxification of the explosive 2,4,6-trinitrotoluene in Arabidopsis: discovery of bifunctional O- and C-glucosyltransferases, Plant J. 56 (2008) 963–974.

[23] A. Gutmann, B. Nidetzky, Enzymatic C-glycosylation: Insights from the study of a complementary pair of plant O- and C-glucosyltransferases, Pure Appl. Chem. 85 (2013) 1865–1877. doi:10.1351/pac-con-12-11-24.

[24] A. Gutmann, B. Nidetzky, Switching between O- and C-Glycosyltransferase through Exchange of Active-Site Motifs, Angew Chem Int Ed. 51 (2012) 12879–12883. doi:10.1002/anie.201206141.

[25] S. Marroun, S. Montaut, S. Marquès, P. Lafite, G. Coadou, P. Rollin, G. Jousset, M. Schuler, A. Tatibouët, H. Oulyadi, R. Daniellou, UGT74B1 from Arabidopsis thaliana as a versatile biocatalyst for the synthesis of desulfoglycosinolates, Org. Biomol. Chem. 14 (2016) 6252–6261. doi:10.1039/c6ob01003b.

[26] J. Stepper, S. Shastri, T.S. Loo, J.C. Preston, P. Novak, P. Man, C.H. Moore, V. Havlicek, M.L. Patchett, G.E. Norris, Cysteine S-glycosylation, a new post-translational modification found in glycopeptide bacteriocins, FEBS Lett. 585 (2011) 645–650. doi:10.1016/j.febslet.2011.01.023.

[27] T.J. Oman, J.M. Boettcher, H. Wang, X.N. Okalibe, W.A. van der Donk, Sublancin is not a lantibiotic but an S-linked glycopeptide, Nat. Chem. Biol. 7 (2011) 78–80. doi:10.1038/nchembio.509.

[28] H. Wang, W.A. van der Donk, Substrate selectivity of the sublancin S-glycosyltransferase, J Am Chem Soc. 133 (2011) 16394–16397. doi:10.1021/ja2075168.

[29] Y.S.Y. Hsieh, B.L. Wilkinson, M.R. O'Connell, J.P. Mackay, J.M. Matthews, R.J. Payne, Synthesis of the Bacteriocin Glycopeptide Sublancin 168 and S-Glycosylated Variants, Org Lett. 14 (2012) 1910–1913. doi:10.1021/ol300557g.

[30] C.D. Grubb, B.J. Zipp, J. Ludwig-Müller, M.N. Masuno, T.F. Molinski, S. Abel, Arabidopsis glucosyltransferase UGT74B1 functions in glucosinolate biosynthesis and auxin homeostasis., Plant J. 40 (2004) 893–908. doi:10.1111/j.1365-313X.2004.02261.x.

[31] J. Kopycki, E. Wieduwild, J. Kohlschmidt, W. Brandt, A.N. Stepanova, J.M. Alonso, M.S. Pedras, S. Abel, C.D. Grubb, Kinetic analysis of Arabidopsis glucosyltransferase UGT74B1 illustrates a general mechanism by which enzymes can escape product inhibition, Biochem. J. 450 (2013) 37–46. doi:10.1042/bj20121403.

[32] S. Yoganathan, S.J. Miller, N-Methylimidazole-catalyzed Synthesis of Carbamates from Hydroxamic Acids via the Lossen Rearrangement, Org. Lett. 15 (2013) 602–605. doi:10.1021/ol303424b.

[33] N. Ohtsuka, M. Okuno, Y. Hoshino, K. Honda, A base-mediated self-propagative Lossen rearrangement of hydroxamic acids for the efficient and facile synthesis of aromatic and aliphatic

primary amines, Org. Biomol. Chem. 14 (2016) 9046–9054. doi:10.1039/C6OB01178K.
[34] M. Jia, H. Zhang, Y. Lin, D. Chen, Y. Chen, Y. Xia, Consecutive Lossen rearrangement/transamidation reaction of hydroxamic acids under catalyst- and additive-free conditions, Org. Biomol. Chem. 16 (2018) 3615–3624. doi:10.1039/C8OB00490K.
[35] V. Lombard, H. Golaconda Ramulu, E. Drula, P.M. Coutinho, B. Henrissat, The carbohydrate-active enzymes database (CAZy) in 2013, Nucleic Acids Res. 42 (2014) D490-5. doi:10.1093/nar/gkt1178.
[36] N. Ibrahim, I. Allart-Simon, G.R. De Nicola, R. Iori, J.-H. Renault, P. Rollin, J.-M. Nuzillard, Advanced NMR-Based Structural Investigation of Glucosinolates and Desulfoglucosinolates, J. Nat. Prod. 81 (2018) 323–334. doi:10.1021/acs.jnatprod.7b00776.
[37] D. Dong, R. Ako, M. Hu, B. Wu, Understanding substrate selectivity of human UDP-glucuronosyltransferases through QSAR modeling and analysis of homologous enzymes., Xenobiotica. 42 (2012) 808–20. doi:10.3109/00498254.2012.663515.
[38] A.-S. Patana, M. Kurkela, M. Finel, A. Goldman, Mutation analysis in UGT1A9 suggests a relationship between substrate and catalytic residues in UDP-glucuronosyltransferases., Protein Eng. Des. Sel. 21 (2008) 537–43. doi:10.1093/protein/gzn030.
[39] K. Nagata, S. Mizukami, Studies on Thiohydroxamic Acids and Their Metal Chelates. II. Structures of Thiohydroxamic Acids, Chem. Pharm. Bull. (Tokyo). 14 (1966) 1255–1262. doi:10.1248/cpb.14.1255.
[40] J. Bezençon, M.B. Wittwer, B. Cutting, M. Smieško, B. Wagner, M. Kansy, B. Ernst, pKa determination by 1H NMR spectroscopy – An old methodology revisited, J. Pharm. Biomed. Anal. 93 (2014) 147–155. doi:10.1016/j.jpba.2013.12.014.
[41] K. Popov, H. Rönkkömäki, L.H.J. Lajunen, Guidelines for NMR measurements for determination of high and low pKa values (IUPAC Technical Report), Pure Appl. Chem. 78 (2006) 663–675. doi:10.1351/pac200678030663.
[42] S.S. Lee, S.Y. Hong, J.C. Errey, A. Izumi, G.J. Davies, B.G. Davis, Mechanistic evidence for a front-side, SNi-type reaction in a retaining glycosyltransferase, Nat Chem Biol. 7 (2011) 631–638. doi:10.1038/nchembio.628.
[43] J.-D. Ye, N.-S. Li, Q. Dai, J.A. Piccirilli, The Mechanism of RNA Strand Scission: An Experimental Measure of the Brønsted Coefficient,βnuc, Angew. Chemie Int. Ed. 46 (2007) 3714–3717. doi:10.1002/anie.200605124.
[44] B.A. Halkier, J. Gershenzon, Biology and biochemistry of glucosinolates, Annu. Rev. Plant Biol. 57 (2006) 303–333.
[45] X. Wang, Structure, mechanism and engineering of plant natural product glycosyltransferases, FEBS Lett. 583 (2009) 3303–3309. doi:10.1016/j.febslet.2009.09.042.

[46] M.S. Macauley, K.A. Stubbs, D.J. Vocadlo, O-GlcNAcase catalyzes cleavage of thioglycosides without general acid catalysis, J. Am. Chem. Soc. 127 (2005) 17202–17203. doi:10.1021/ja0567687.